

Ocular hypotension, actin stress fiber disruption and phagocytosis increase by RKI-1447, a Rho-kinase inhibitor

Yalong Dang, MD, Ph.D.¹, Chao Wang, MB^{1,2}, Priyal Shah, BSc^{1,3}, Susannah Waxman, BSc¹, Ralitsa T. Loewen, MD¹, and Nils A. Loewen, MD, Ph.D.^{*1}

1. Department of Ophthalmology, University of Pittsburgh School of Medicine, Pittsburgh, Pennsylvania, United States of America

2. Department of Ophthalmology, Xiangya Hospital, Central South University, Changsha, Hunan, People's Republic of China

3. Institute of Ophthalmology and Visual Science, Rutgers New Jersey Medical School, Newark, New Jersey, United States of America.

*** Corresponding author**

Nils A. Loewen, MD, Ph.D.

203 Lothrop St, Suite 819, Pittsburgh, PA 15213

Email: loewen.nils@gmail.com, Phone (fax): 412-605-1541

Abstract

Objective: The Rho GTPase/Rho kinase pathway is an important target in glaucoma treatment. This study investigated the hypotensive effect of RKI-1447, a Rho kinase inhibitor developed for cancer treatment, in a porcine ex vivo pigmentary glaucoma model.

Materials and Methods: Twenty-eight fresh porcine anterior chambers were perfused with pigment medium (1.67×10^7 pigment particles/ml) for 48 hours before being subjected to the RKI-1447 (n=16) or the vehicle control (n=12). Another twelve eyes with normal medium perfusion served as the control. The intraocular pressure (IOP) was recorded at two-minute intervals and the outflow facility was calculated. To investigate the intracellular mechanism of the IOP reduction, primary trabecular meshwork cells were exposed to RKI-1447 or the vehicle control and then analyzed for changes in cytoskeleton, motility, and phagocytosis.

Results: Compared to the baseline, the perfusion of pigment caused a significant increase in IOP in the RKI-1447 group ($P=0.003$) at 48 hours. Subsequent treatment with RKI-1447 significantly reduced IOP from 20.14 ± 2.59 mmHg to 13.38 ± 0.91 mmHg ($P=0.02$). Pigment perfusion reduced the outflow facility from 0.27 ± 0.03 at baseline to 0.18 ± 0.02 at 48 hours ($P<0.001$). This was partially reversed with RKI-1447. RKI-1447 exhibited no apparent changes in the micro- or macroscopic appearance, including histology. Primary TM cells exposed to RKI-1447 showed a significant disruption of the actin cytoskeleton both in the presence and absence of pigment exposure ($P<0.001$) but no effect on TM migration was observed. Pigment-treated TM cells exhibited a reduction in TM phagocytosis, which RKI reversed.

Conclusions: RKI-1447 is a novel ROCK inhibitor that significantly reduces IOP by disrupting TM stress fibers and increasing TM phagocytosis. These features may make it especially useful for the treatment of secondary glaucomas with an increased phagocytosis load but also for other open angle glaucomas.

Introduction

The ocular hypertension that is frequently observed in glaucoma patients exhibits a complex pathomechanism that remains incompletely understood¹. The intraocular pressure (IOP) remains the single most important modifiable variable in glaucoma treatment². Current topical medications for glaucoma typically increase the uveoscleral outflow of aqueous humor (prostaglandin analogues) or reduce aqueous humor production (beta-adrenergic blockers, alpha-adrenergic agonists, carbonic anhydrase inhibitors). The only drugs that increase the conventional outflow that are readily available at the time of this writing are cholinergic agonists who have miosis and ciliary spasm as significant side effects² although NO donors are on the horizon that relax the TM to increase outflow³. In the present study we examine the hypotensive effect of RKI-1447, which was originally introduced as an anti-tumor agent in breast cancer treatment⁴.

The Rho-associated protein kinase (ROCK) is part of the serine-threonine kinases that act on the cytoskeleton to regulate the movement and shape of cells. It plays a central role in biological functions such as stress-fibre formation and contraction, cell adhesion, migration and invasion, transformation, phagocytosis and apoptosis, cytokinesis and mitosis as well as differentiation^{5,6}. Previous studies found that ROCK is expressed in the TM and upregulated in the optic nerve head of glaucomatous eyes^{7,8}. Honjo and colleagues found that ROCK inhibitor Y-27632 increased the outflow facility in a dose-dependent manner in rabbit eyes⁹. The investigators suggested that the hypotensive effect may result from a disruption of actin bundles and reduction in the focal adhesion of TM cells⁹. Similarly, recent studies found that ROCK inhibitors disrupt tight junctions thereby increasing the permeability of Schlemm's canal endothelium^{10,11} in addition to decreasing the episcleral venous pressure¹².

Ripasudil (K-115) was the first approved ROCK inhibitor for glaucoma^{13,14}. Two randomized trials involving 413 Japanese primary open-angle glaucoma patients found that Ripasudil achieved an average of 0.4-1.6 mmHg higher IOP reduction than the administration of timolol or latanoprost alone¹⁵. Phase II/III trials that aim to investigate the IOP-lowering effect of four different ROCK inhibitors (AMA0076¹⁶, AR-13324¹⁷, K-115¹⁴ and PG-324¹⁸) are currently in process. Several trials that employed functionally and structurally similar compounds were discontinued due to the low therapeutic efficiency and high incidence of adverse events¹⁹.

First characterized by Patel et al. in 2012⁴, RKI-1447 inhibits the type I kinase by binding to the ATP binding site through interaction with the Asp-Phe-Gly motif and hinge region (**Figure 1**)^{4,20}. In vitro, it selectively inhibits the ROCK1/2-mediated actin stress fiber formation at the low level of IC-50 (14.5nM and 6.2nM for ROCK1 and ROCK2, respectively²¹) following lysophosphatidic acid stimulation. Unlike other ROCK inhibitors, RKI-1447 does not exhibit cross-reactivity with AKT, MEK, PKA, and PKG signaling, even at a high concentration of up to 10 μ M^{4,21}, reducing the risk of side effects. Recently, our group developed an ex vivo pigmentary glaucoma model that exhibited a IOP elevation, a typical TM stress fiber formation, and a reduction in TM phagocytosis^{22,23}. In this paper, we examine the ocular hypotensive effect of RKI-1447 in an ex vivo anterior chamber perfusion model and investigate its possible mechanisms.

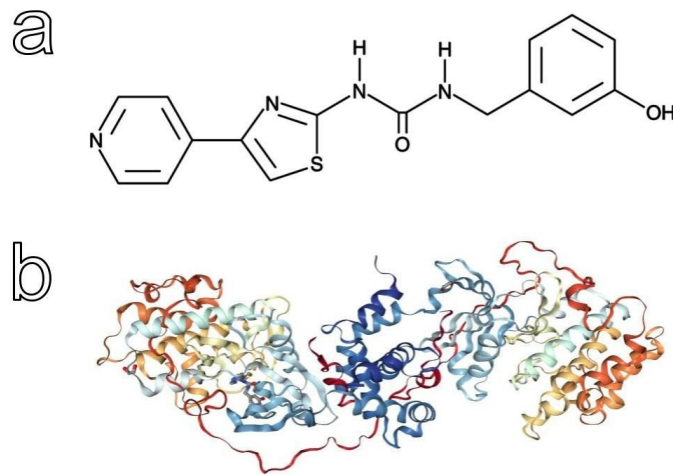


Figure 1. Molecular structure of RKI-1447. RKI-1447 is an ATP site-targeting Rho kinase inhibitor with an IC₅₀ of 14.5 nM and 6.2 nM for ROCK1 and ROCK2, respectively (a). It has a crystal structure and works by interacting with the Asp-Phe-Gly motif and hinge region of ROCKs (b).

Materials and Methods

Pig eye perfusion, pigmentary glaucoma model, and RKI-1447 intervention

No live animals were involved in the study and the eyes were obtained from a local abattoir. As a result no Institutional Animal Care and Use Committee protocol was required. The setup of the porcine eye perfusion system followed our prior protocols^{22,24–26}. Briefly, 40 freshly enucleated pig eyes were obtained from a local slaughterhouse (Thoma Meat Market, Saxonburg, PA) and processed within two hours of sacrifice. After the removal of extraocular tissues, the eyes were disinfected in a 5% povidone-iodine ophthalmic solution (betadine 5%; Alcon, Fort Worth, TX, USA) for two minutes, washed three times with PBS, and hemisected. The anterior chambers were then mounted on the perfusion dishes and subsequently underwent continuous perfusion with 1% FBS supplemented with DMEM and antibiotics at a constant rate of 3 μ l per min.

Once the baseline IOPs were obtained, 28 of the 40 eyes were perfused with the pigment medium for 48 hours (1.67 \times 10⁷ pigment particles/ml) before being subjected to the RKI-1447 (n=16) or the vehicle control (n=12). For the RKI-1447 group, RKI-1447 was diluted into the pigment medium to a final concentration of 1 μ M before the solution was perfused into the eyes. For the vehicle control, the eyes were continuously perfused with the same pigment medium. A total of 12 of the 40 samples without the pigment perfusion and the RKI-1447 served as the normal control. IOPs were measured using a pressure transducer at a two-minute interval.

Production of pigment dispersion particles

Pigment particles for pigment dispersion were produced as previously described using a freeze-thaw protocol²⁵. In brief, ten porcine irises were sealed in a 50-ml tube, frozen at a temperature of -80° for 2 hours, then thawed at room temperature. After two cycles of freeze-thaw, 15 ml of PBS was added to the tube. By

pipetting up and down 100 times with a 3 ml Pasteur pipette, the pigment particles were shed from the irises. They were then collected and centrifuged at 3000 rpm for 15 min. The supernatant was discarded, and the pigment pellet was resuspended and centrifuged again at the same settings. Finally, the pigment particles were resuspended in 4 ml of phosphate-buffered saline (PBS) as the stock solution and titered using a hemocytometer (#1490, Hausser Scientific, Horsham, PA) at 1000-fold dilution as per the method previously described²⁵.

Histology

At the conclusion of the experiments, the chambers were dismantled, washed with PBS, fixed with 4% PFA for 24 hours and paraffin embedded. The samples were sectioned at 6-micron thickness, followed by staining with Hematoxylin and Eosin.

Primary TM culture

Primary porcine TM cells were purified and characterized by our previous protocol²⁵. A porcine anterior chamber was dissected as above. After removing the extra sclera and cornea, the entire TM stripes were sectioned into 1 mm X 1 mm pieces and cultured in a T75 flask with TM-culturing medium (5% FBS supplemented with OptiMEM and antibiotics). Primary TM cells started to migrate onto the flask on day four and formed clones. The cells were passaged at 80% confluence and replated at a 1:3 ratio. We characterized these cells by immunostaining with a combination of TM specific antibodies (alpha smooth muscle actin [alpha-SMA] antibody, matrix gla protein [MGP] antibody and aquaporin 1 [AQP1]) and an in vitro phagocytic assay. To avoid transformation and differentiation, only the cells within the first four passages were used.

Immunostaining

For further characterization, we plated these primary cells onto 10 mm X 10 mm glass slides and fixed them with 4% PFA at 80% confluence. This was followed by washing with PBS three times and incubation with the primary antibody overnight at 4°. The primary antibodies were goat polyclonal anti-MGP antibodies (1:100 dilution, sc-32820, Santa Cruz, Dallas, Texas), rabbit polyclonal anti alpha-SMA (1:100, ab5694, Abcam, Cambridge, MA) and rabbit polyclonal anti-AQP1 antibodies (1:100, Sc-20810, Santa Cruz, Dallas, Texas). After three rinses in PBS, a mixture of secondary antibodies (donkey-anti-goat Alexa Fluor® 647 [1: 200, ab150131, Abcam, Cambridge, MA] and goat anti-rabbit Alexa Fluor® 488 [1:1000, A27034, Thermo Scientific, Waltham, MA]) was incubated with the cells for 45 minutes at room temperature. The cell nuclei were counterstained with DAPI (1: 1000, D1306, Thermo Fisher Scientific, Waltham, MA) for 15 minutes. Images were taken using an upright laser scanning confocal microscope at 400x magnification (BX61, Olympus, Tokyo, Japan).

To quantify the stress fiber formation, the cells were fixed with 4% PFA for 24 hours before being stained with Alexa Fluor® 488 Phalloidin for 30 minutes (1:20, A12379, Thermo Scientific, Waltham, MA). The cell nuclei were labeled with 4',6-diamidino-2-phenylindole (DAPI). Images were acquired using the upright confocal microscope at the same settings as those used to take images of the cell nuclei. Ten randomized visual fields were chosen to quantify the percentages of cells with stress fibers for each group.

TM motility assay

The in vitro TM cell motility was using a scratch assay with a minor modification²⁷. In brief, 2×10^5 of primary TM cells were seeded into each well of a six-well plate and cultured in an environmental chamber that was equipped with a digital camera and image acquisition software. After reaching 80% confluency, the cells were treated with pigment particle at a concentration of 1.67×10^7 particles/ml for 24 hours. A 10 μ l pipette tip was used to create a cell-free scratch that had a consistent width. Following that, RKI-1447 (final concentration: 1 μ M) or vehicle was applied. Pictures from ten positions of each well were acquired at a two-hour interval, up to 20 hours. The numbers of TM cells moved into the cell-free scratch were counted.

TM phagocytosis assay

The phagocytic activity of the primary TM cells was measured by flow cytometry using fluorescence microsphere ingestion test²⁵. 2×10^5 primary TM cells were seeded into each well of a six-well plate and underwent the pigment exposure (final concentration: 1.67×10^7 particles/ml) or vehicle treatment for seven days. Half of the cells were then treated with RKI-1447 (final concentration: 1 μ M) for 24 hours while the rest underwent the sham treatment. To quantify the phagocytic activity, the cells were incubated with 0.5-micron fluorescence microsphere at 5×10^8 /ml at 37 degrees for 1 hour. After washing thoroughly with PBS, the cells were dissociated with trypsin and resuspended in 200 μ l PBS for flow cytometry. The percentage of cells ingested with microspheres was determined.

Statistics

Quantitative data were presented as the mean \pm standard error and processed by PASW 18.0 (SPSS Inc., Chicago, IL, USA). A paired t-test was used to compare the IOP responses from the baseline. Other quantitative data were compared by one-way ANOVA. A $p \leq 0.05$ was considered to be statistically significant.

Results

IOP reduction and increase of outflow facility

The baseline IOPs among these three groups were comparable (10.32 \pm 0.82 mmHg in the pigment group versus 12.21 \pm 1.06 mmHg in the RKI-1447 group and 10.21 \pm 1.15 mmHg in the control group, $P=0.291$). Compared to each baseline, the intracameral perfusion of pigment particles resulted in a significant IOP elevation in the pigment group ($P=0.038$) and the RKI-1447 group ($P=0.003$) at 48 hours, while IOPs in the control group remained unchanged ($P=0.108$). RKI-1447 significantly reduced IOP from 20.14 \pm 2.59 mmHg to 13.38 \pm 0.91 mmHg at 60 hours then remained at a low level throughout the study. In contrast, the IOP in the pigment group remained high in comparison to its baseline (all $P < 0.05$). At all time points after RKI-1447, the IOP in the RKI-1447 group exhibited no statistical difference compared to the control (all $P > 0.05$); however, both were significantly lower than those in the pigment group (all $P < 0.05$) (**Figure 2 A**).

Because the episcleral venous pressure is close to zero in the perfusion system, the outflow facility is inversely correlated with IOP. In the current study, the baseline outflow facility exhibited no difference across the three

groups ($P=0.316$). Pigment perfusion caused a significant reduction in the outflow facility in the RKI-1447 group from 0.27 ± 0.03 at the baseline to 0.18 ± 0.02 at 48 hours ($P<0.001$), while RKI-1447 partially reversed this effect by 14.57% to 48.35% at the follow-up time points. In contrast, the outflow facility in the pigment group continuously decreased from a baseline of 0.31 ± 0.03 to 0.15 ± 0.01 at the end of the study (all $P<0.05$, compared to its baseline). In the control group, the outflow facility exhibited a slight decrease as the time elapsed (**Fig. 2 B**).

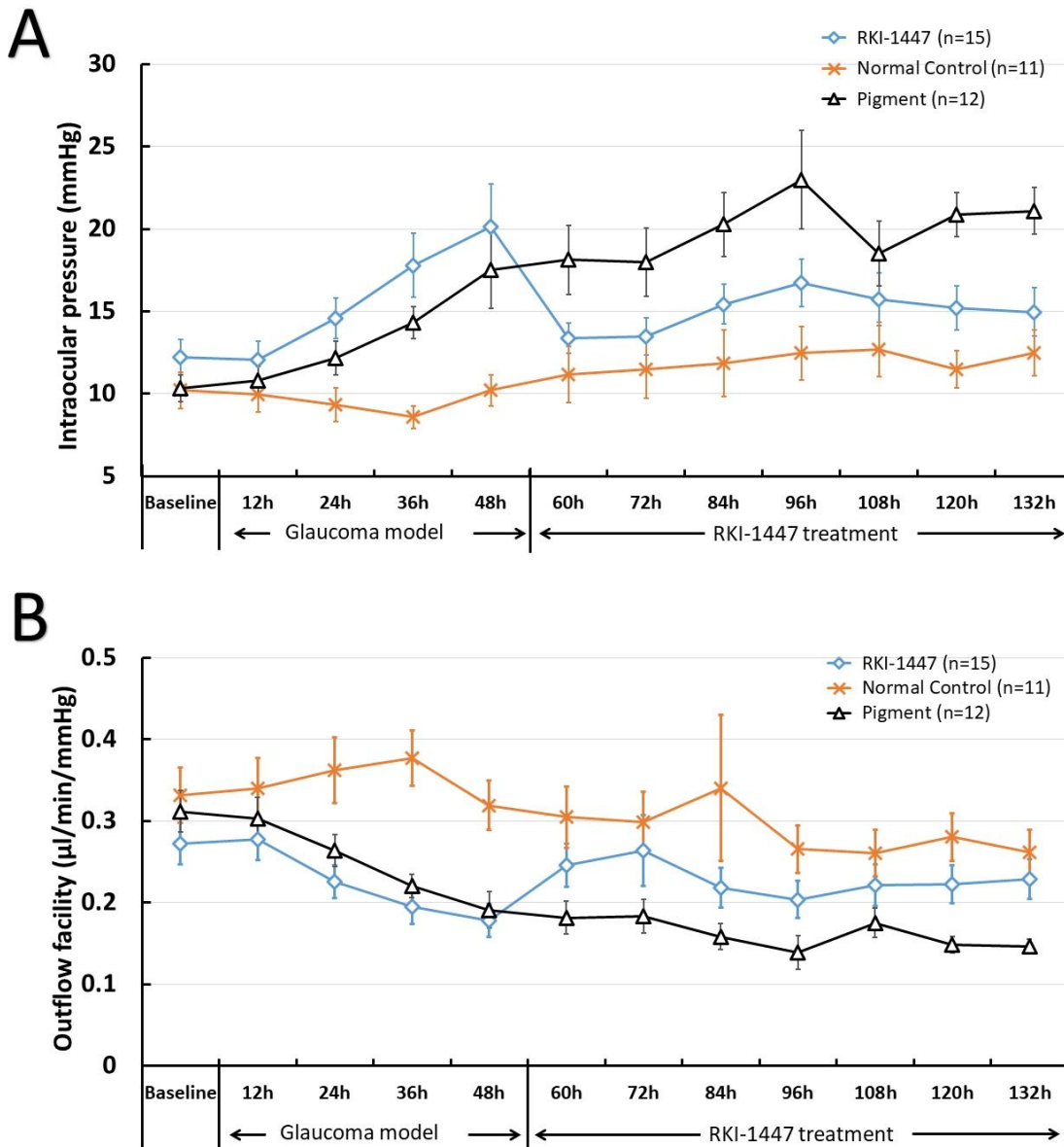


Figure 2. The changes of intraocular pressure and outflow facility by RKI-1447 treatment. IOP at different time points is shown. Measurements taken after 48 hrs. after pigment injection revealed that there was a significant increase in IOP in the RKI-1447 ($P=0.003$) and the pigment groups ($P=0.038$) from their baseline measurements. After treatment with RKI-1447, the IOP of the RKI-1447 group decreased significantly from 20.14 ± 2.59 mmHg to 13.38 ± 0.91 , while the pigment group remained significantly higher than its baseline (all $P<0.05$) (**A**). In the RKI-1447 group, the injection of pigment resulted in a significant reduction in outflow facility when measured at 48 hours ($P<0.001$), which was partially

reversed after RKI-1447 treatment. In the pigment group, the outflow facility was significantly reduced at all time points in comparison to baseline (all $P < 0.05$) **(B)**.

TM histology

Normal TM exhibits a light-pigmented, multilayer, strainer-like structure connected with opening Schlemm's canals **(Figure 3a)**. Consistent with our previous findings^{22,25}, pigment perfusion resulted in an increased pigmentation in the TM, while most of the pigment particles seemed to be phagocytosed by TM cells without physically obstructing the TM **(Figure 3b)**. RKI-1447 treatment exhibited no apparent changes in TM histology **(Figure 3c)**.

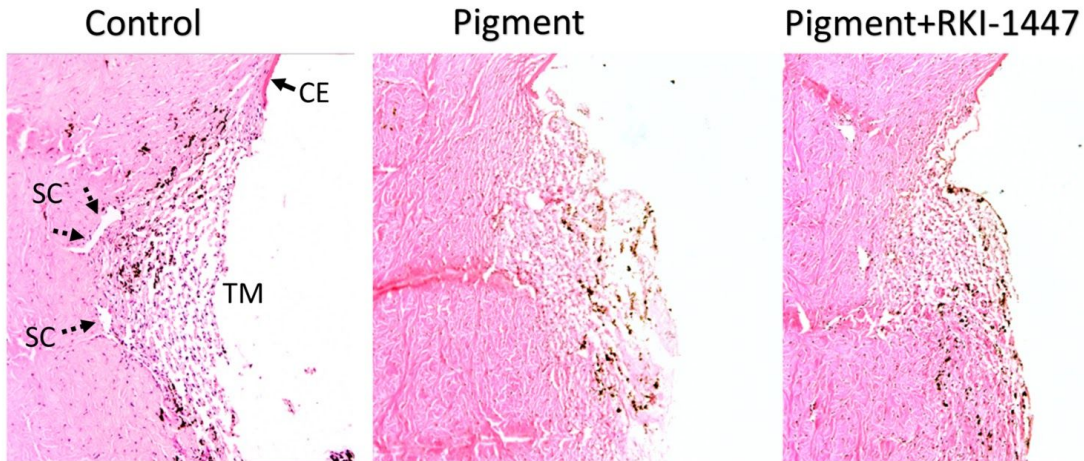


Figure 3. TM histology. The TM in the control group presented as a lightly-pigmented strainer-like tissue, consisting of parallel collagen beams with TM cells **(left)**. Perfusion with pigment particles resulted in an increase in TM pigmentation **(middle)** and was equal to RKI-1447 exposed eyes **(right)**. TM: trabecular meshwork. SC: Schlemm's canal-like segments of the porcine angular aqueous plexus. CE: corneal endothelium.

Disruption of TM actin stress fibers

The primary TM cells showed an elongated morphology **(Figure 4a)**, active phagocytosis **(Figure 4b)**, and were positive for TM-specific markers alpha-SMA, AQP1, and MGP **(Figures 4c and 4d)**. Pigment exposure did not cause an apparent morphological change in TM cells²⁵ **(Figures 4e and 4g)**, while RKI-1447 stimulated a cell body contraction within minutes, in the presence or absence of pigment exposure **(Figures 4f and 4h)**.

F-actin cytoskeleton labeling with Alexa Fluor® 488 Phalloidin, showed a baseline of 32.57 ± 2.66 % actin stress fibers in normal TM cells, compared to 67.13 ± 4.00 % in the pigment-exposed TM cells ($P < 0.001$) **(Figures 4i and 4k)**. RKI-1447 abolished these stress fibers, both in normal TM cells (2.57 ± 0.86 % versus 32.57 ± 2.66 %, $P < 0.001$) and pigment-exposed TM cells (2.51 ± 0.71 % versus 67.13 ± 4.00 %, $P < 0.001$) **(Figures 4j, 4i, and 4m)**.

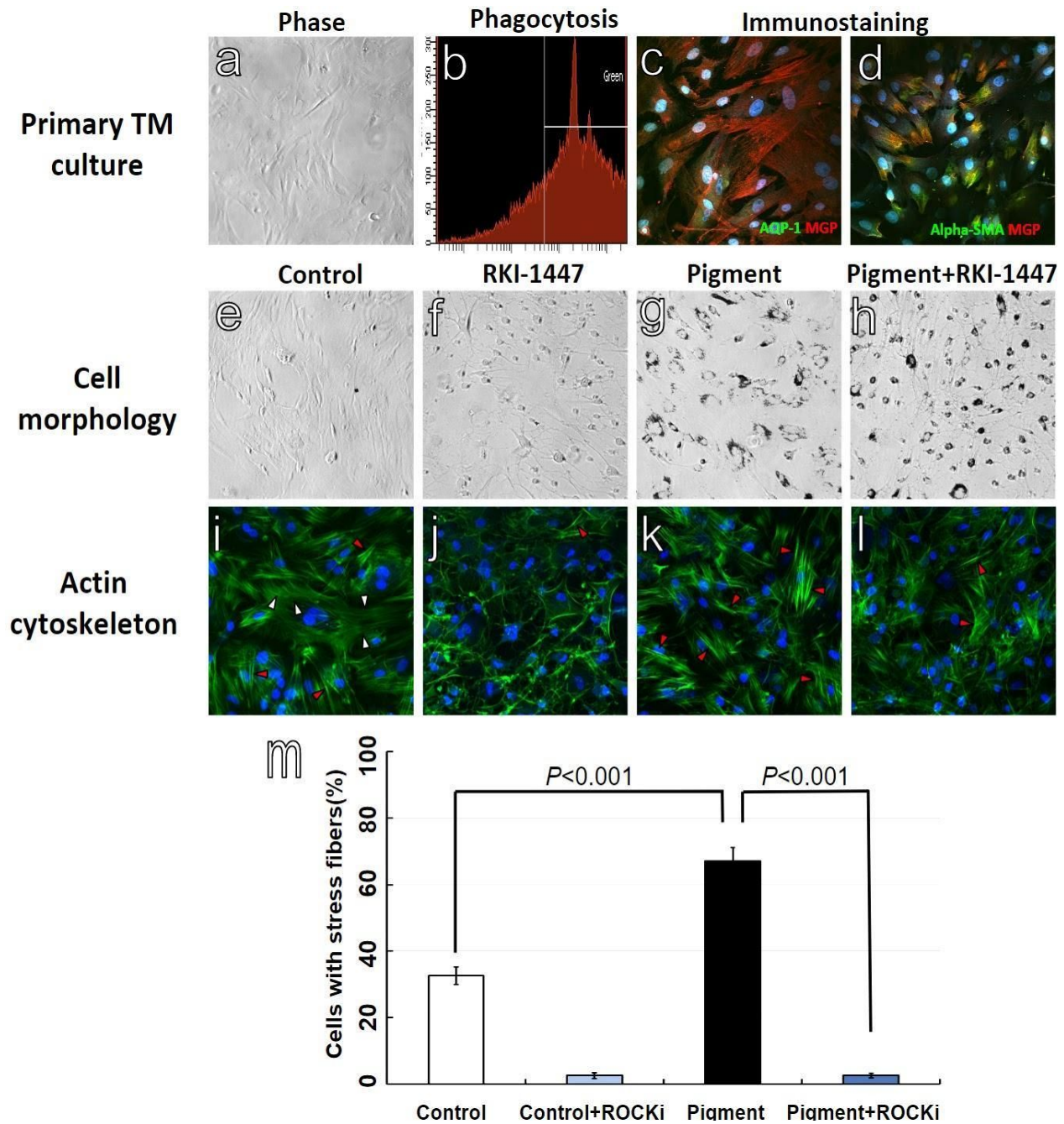


Figure 4. Primary TM culture, cell morphology, and actin cytoskeleton. Primary porcine TM cells were elongated (Figure 3a) and had an active phagocytic activity (Figure 3b). They tested positive for the TM-specific markers (Figures 3c and 3d) AQP1, alpha-SMA, and MGP. Pigment exposure did not stimulate a significant morphological change. Cells contracted following RKI-1447 (Figures 3e, 3f, 3g, and 3h). RKI-1447 significantly disrupted the actin cytoskeleton regardless of presence or absence of pigment ($P < 0.001$) (Figures 3i, 3j, 3k, 3l, and 3m).

TM motility

Since changes in TM movement have been reported in studies of glaucomatous eyes^{25,28}, we tested the effect of RKI-1447 on TM motility using a modified scratch assay. As shown in Figure 5, the pigment exposure statistically decreased the numbers of migrating TM cells (60.83 ± 3.46 in the normal control versus 31.75 ± 3.36 cells in the pigment treated group, $P < 0.001$) while RKI-1447 seemed to have no effect on the TM migration,

either for the normal TM cells or the pigment-treated TM cells ($P=0.091$ and $P=0.398$, compared to each baseline).

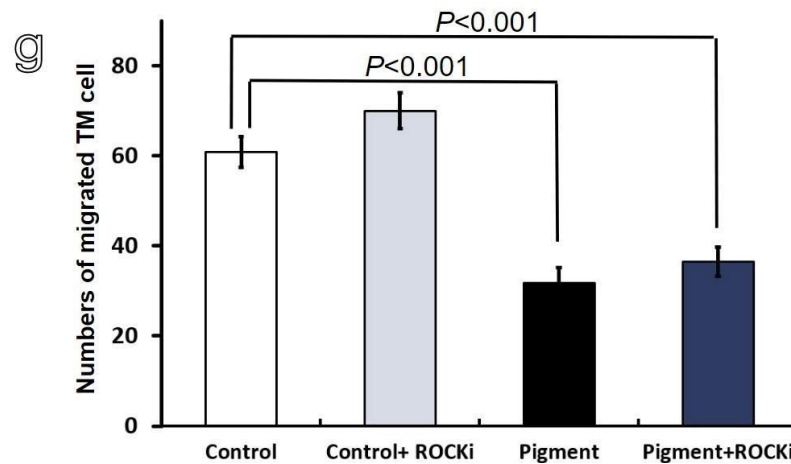
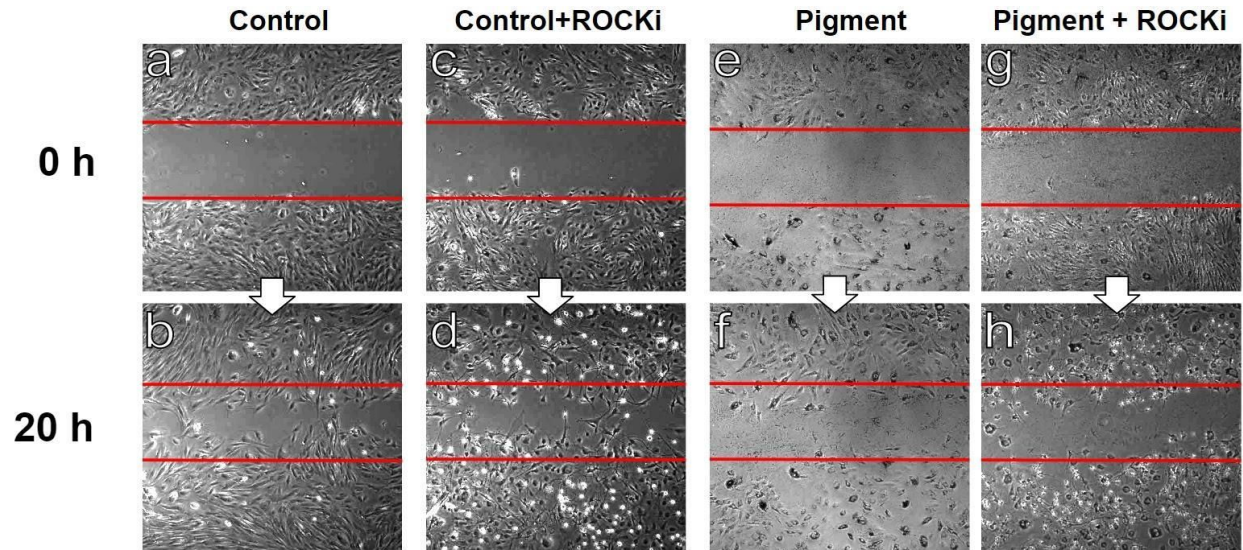


Figure 5. RKI-1447 did not effect TM motility. The motility of TM cells was measured using a scratch assay with minor modification. Compared to the normal control, pigment exposure resulted in a significant reduction in the number of migrating TM cells (60.83 ± 3.46 in the control versus 31.75 ± 3.36 cells in the pigment group, $P < 0.001$). RKI-1447 had no significant effect on the TM migration, either for the normal TM cells ($P=0.091$) or the pigment-treated TM cells ($P=0.398$) in comparison to the baseline.

Consistent with our previous results^{22,25}, pigment exposure caused a reduction in TM phagocytosis by 10.31% while RKI-1447 reversed this effect and increased it to 111.52% in comparison to the normal baseline.

Discussion

Pigmentary glaucoma (PG) is a common type of secondary open-angle glaucoma with an incidence of 1.4/100,000^{29,30}. A readily recognisable feature of this disease is the wide dispersion of pigment in intraocular tissues, especially on the corneal endothelium and in trabecular meshwork³¹. Our previous study in a porcine eye perfusion model suggested that iris pigment particles induced TM stress fibers, reduced TM phagocytosis,

adhesion, and motility, and resulted in a significant IOP elevation²⁵. In the current study, we found that RKI-1447, a ROCK1/ROCK2 inhibitor, efficiently reduced the IOP by 33.58% and increased the outflow facility by 38.25% in the same pigmentary glaucoma model. Our in vitro results further revealed that these changes might result from the extensive disruption of TM actin stress fibers.

In the current study, we utilized a porcine anterior segment perfusion model that mimicks the TM changes and IOP phenotype of human PG to examine the hypotensive effect of RKI-1447, an oncology drug used in breast cancer⁴. Pigment dispersion caused a significant IOP elevation at the 48-hour time interval, while RKI-1447 partially reversed this effect throughout the study. The TM regulates aqueous outflow by changing its cytoskeleton, stiffness, cell adhesion, migration, contraction, and phagocytosis^{32,33}, and ROCK signaling plays a central role in these processes^{7,34}.

A close interaction between the actin cytoskeleton reorganization, cell or extracellular matrix stiffness, and aqueous outflow facility was observed^{35,36}. Consistent with our previous work²⁵, only a small portion of stress fibers formed in the normal TM culture while the pigment exposure increased it by 2.06-fold. Actin stress fibers provided a dominant contribution to both cell stiffness and the stiffness of the extracellular matrix^{35,37,38} that directly affected aqueous outflow facility³⁶. Gavara et al. also found that the presence of aligned and thick stress fibers in the cell periphery gave rise to reinforced cell stiffness³⁹. In general, factors that induce stress fiber formation increase TM stiffness and decrease outflow facility. For example, senescence and aging, a risk factor for primary open-angle glaucoma, has increases the stress fiber formation and TM stiffness⁴⁰. In a different study, dexamethasone, an inducer of cross-linked actin network^{41,42}, increased the stiffness of primary TM cells and extracellular matrix twofold and fourfold, respectively, after three days³⁸, and caused an IOP elevation in an ex vivo perfusion model of human eyes⁴². In contrast, numerous reagents have been found to disrupt actin stress fiber and exhibit an ocular hypotensive effect. For instance, Y27632, but not isoproterenol, pilocarpine, or nifedipine, significantly have been found to abolish cyclic stress-induced stress fiber and reverse the elevation of intrachamber pressure⁴³. In another study, Rao et al. showed that Y27632 increased the outflow facility by 40%-80% in pig eyes⁴³. Other molecules that target the myosin light chain and its kinase have exhibited a similar effect⁴⁴⁻⁴⁶. In the current study, RKI-1447 significantly disrupted the stress fiber in the pigment-treated TM cells, and the IOP-reducing effect could be at least partially attributed to this.

As is the case with other ROCK inhibitors^{9,46,47}, we found that RKI-1447 caused a significant contraction of TM cells. These cells exhibited a round shape and were less adhesive. We also quantified TM motility using live cell imaging. The results suggested that the pigment exposure resulted in a significant reduction in TM migration; however, it seemed unaffected by RKI-1447, indicating that the IOP-lowering effect might not be directly related to TM motility.

Phagocytosis is driven by a well coordinated rearrangement of the actin cytoskeleton^{48,49}. It maintains the homeostasis of trabecular outflow by removing the cell debris and melanin from outflow tracts^{32,50}. A reduction in TM phagocytosis has been observed in various types of glaucoma or glaucoma models. For instance, human eye perfusion with dexamethasone for 21 days resulted in a 57% decrease of TM phagocytosis without causing a significant loss in TM cells⁵¹. SWAP70, VASP, and WASP, were believed to play an essential role in this process⁵². Consistent with previous studies^{22,51}, we found a 10.31% reduction in TM phagocytosis following pigment exposure, while RKI-1447 increased it to 111.52% in comparison to the control.

Our study has a number of limitations. First, the anatomical difference between the human and the porcine outflow tract and their angular aqueous plexus is significant⁵³. Domestic pigs, even ones used as breeders, are not known to develop glaucoma. A study by Camras et al. suggested that TM stiffness was correlated with outflow facility in human eye perfusion but not in the pig specimens⁵⁴. Second, this ex vivo study does not account for important factors that can only be examined *in vivo.*, this study focused on the effect of RKI-1447 on the TM but it is possible that dilation of post-trabecular outflow tract structures also exhibit a hypotensive effect in human open angle glaucoma where a high resistance of often remains after trabecular ablation⁵⁵⁻⁵⁸.

In conclusion, the ROCK inhibitor RKI-1447 reduced IOP in a pigmentary glaucoma model while disrupting TM stress fibers and increasing phagocytosis.

Acknowledgements

We acknowledge support from NIH CORE Grant P30 EY08098 to the Department of Ophthalmology, from the Eye and Ear Foundation of Pittsburgh, and from an unrestricted grant from Research to Prevent Blindness, New York, NY. We thank Vappingo (Moo Media Limited, UK) for editing the English text of this manuscript.

References

1. Janssen SF, Gorgels TGMF, Ramdas WD, et al. The vast complexity of primary open angle glaucoma: disease genes, risks, molecular mechanisms and pathobiology. *Prog Retin Eye Res.* 2013;37:31-67.
2. Weinreb RN, Aung T, Medeiros FA. The pathophysiology and treatment of glaucoma: a review. *JAMA.* 2014;311(18):1901-1911.
3. Weinreb RN, Ong T, Scassellati Sforzolini B, et al. A randomised, controlled comparison of latanoprostene bunod and latanoprost 0.005% in the treatment of ocular hypertension and open angle glaucoma: the VOYAGER study. *Br J Ophthalmol.* December 2014:bjophthalmol - 2014.
4. Patel RA, Forinash KD, Pireddu R, et al. RKI-1447 is a potent inhibitor of the Rho-associated ROCK kinases with anti-invasive and antitumor activities in breast cancer. *Cancer Res.* 2012;72(19):5025-5034.
5. Riento K, Ridley AJ. Rocks: multifunctional kinases in cell behaviour. *Nat Rev Mol Cell Biol.* 2003;4(6):446-456.
6. Katoh K, Kano Y, Ookawara S. Rho-kinase dependent organization of stress fibers and focal adhesions in cultured fibroblasts. *Genes Cells.* 2007;12(5):623-638.
7. Wang J, Liu X, Zhong Y. Rho/Rho-associated kinase pathway in glaucoma (Review). *Int J Oncol.* 2013;43(5):1357-1367.
8. Goldhagen B, Proia AD, Epstein DL, Rao PV. Elevated levels of RhoA in the optic nerve head of human eyes with glaucoma. *J Glaucoma.* 2012;21(8):530-538.
9. Honjo M, Tanihara H, Inatani M, et al. Effects of rho-associated protein kinase inhibitor Y-27632 on intraocular pressure and outflow facility. *Invest Ophthalmol Vis Sci.* 2001;42(1):137-144.
10. Kameda T, Inoue T, Inatani M, et al. The Effect of Rho-Associated Protein Kinase Inhibitor on Monkey Schlemm's Canal Endothelial Cells Effects of ROCK Inhibitor on Schlemm's Canal Cells. *Invest Ophthalmol Vis Sci.* 2012;53(6):3092-3103.
11. Kaneko Y, Ohta M, Inoue T, et al. Effects of K-115 (Ripasudil), a novel ROCK inhibitor, on trabecular meshwork and Schlemm's canal endothelial cells. *Sci Rep.* 2016;6:19640.
12. Kiel JW, Kopczynski CC. Effect of AR-13324 on episcleral venous pressure in Dutch belted rabbits. *J Ocul Pharmacol Ther.* 2015;31(3):146-151.
13. Garnock-Jones KP. Ripasudil: first global approval. *Drugs.* 2014;74(18):2211-2215.
14. Tanihara H, Inoue T, Yamamoto T, et al. One-year clinical evaluation of 0.4% ripasudil (K-115) in patients with open-angle glaucoma and ocular hypertension. *Acta Ophthalmol.* 2016;94(1):e26-e34.
15. Tanihara H, Inoue T, Yamamoto T, et al. Additive Intraocular Pressure-Lowering Effects of the Rho Kinase Inhibitor Ripasudil (K-115) Combined With Timolol or Latanoprost: A Report of 2 Randomized Clinical Trials. *JAMA Ophthalmol.* 2015;133(7):755-761.
16. Multiple Dose-parallel-group Study of AMA0076 in Patients With Primary Open-Angle Glaucoma or Ocular Hypertension - Full Text View - ClinicalTrials.gov. <https://clinicaltrials.gov/ct2/show/NCT02136940>.

Accessed September 7, 2017.

17. Bacharach J, Dubiner HB, Levy B, Kocczynski CC, Novack GD, AR-13324-CS202 Study Group. Double-masked, randomized, dose-response study of AR-13324 versus latanoprost in patients with elevated intraocular pressure. *Ophthalmology*. 2015;122(2):302-307.
18. Double-masked Study of PG324 Ophthalmic Solution in Patients With Open-angle Glaucoma or Ocular Hypertension - Full Text View - ClinicalTrials.gov. <https://clinicaltrials.gov/ct2/show/NCT02674854>. Accessed September 7, 2017.
19. Wang SK, Chang RT. An emerging treatment option for glaucoma: Rho kinase inhibitors. *Clin Ophthalmol*. 2014;8:883-890.
20. Martin MP, Zhu J-Y, Schonbrunn E. Rho-associated protein kinase 1 (ROCK 1) IN COMPLEX WITH RKI1447. 2012. doi:10.2210/pdb3twj/pdb.
21. RKI-1447 | ROCK inhibitor | Read Reviews & Product Use Citations. <http://www.selleckchem.com/products/rki-1447.html?gclid=Cj0KEQjw3MPNBRDj0Yztg4LGvOcbEiQA5hTrH0RIVz8jg86KuAdDjRNteNbuGISVI77ZSILD2KVnPkAarcO8P8HAQ>. Accessed September 7, 2017.
22. Dang Y, Waxman S, Wang C, Loewen RT, Loewen NA. Intraocular pressure elevation precedes a phagocytosis decline in a model of pigmentary glaucoma. *bioRxiv*. August 2017:175695. doi:10.1101/175695.
23. Dang Y, Waxman S, Wang C, Loewen RT, Sun M, Loewen N. Trabecular Meshwork Failure In A Model Of Pigmentary Glaucoma. *bioRxiv*. March 2017:118448. doi:10.1101/118448.
24. Dang Y, Waxman S, Wang C, et al. *Freeze-Thaw Decellularization of the Trabecular Meshwork in an Ex Vivo Eye Perfusion Model*. PeerJ Preprints; 2017. doi:10.7287/peerj.preprints.2736v1.
25. Dang Y, Waxman S, Wang C, Loewen RT, Sun M, Loewen N. A porcine ex vivo model of pigmentary glaucoma. *bioRxiv*. August 2017:118448. doi:10.1101/118448.
26. Loewen RT, Roy P, Park DB, et al. A Porcine Anterior Segment Perfusion and Transduction Model With Direct Visualization of the Trabecular Meshwork. *Invest Ophthalmol Vis Sci*. 2016;57(3):1338-1344.
27. Wang G-Q, Dang Y-L, Huang Q, et al. In Vitro Evaluation of the Effects of Intraocular Lens Material on Lens Epithelial Cell Proliferation, Migration, and Transformation. *Curr Eye Res*. 2017;42(1):72-78.
28. Hogg P, Calthorpe M, Batterbury M, Grierson I. Aqueous humor stimulates the migration of human trabecular meshwork cells in vitro. *Invest Ophthalmol Vis Sci*. 2000;41(5):1091-1098.
29. Siddiqui Y, Ten Hulzen RD, Cameron JD, Hodge DO, Johnson DH. What is the risk of developing pigmentary glaucoma from pigment dispersion syndrome? *Am J Ophthalmol*. 2003;135(6):794-799.
30. Ritch R, Steinberger D, Liebmann JM. Prevalence of pigment dispersion syndrome in a population undergoing glaucoma screening. *Am J Ophthalmol*. 1993;115(6):707-710.
31. Qing G, Wang N, Tang X, Zhang S, Chen H. Clinical characteristics of pigment dispersion syndrome in Chinese patients. *Eye*. 2009;23(8):1641-1646.
32. Llobet A, Gasull X, Gual A. Understanding trabecular meshwork physiology: a key to the control of

intraocular pressure? *News Physiol Sci*. 2003;18:205-209.

33. Abu-Hassan DW, Acott TS, Kelley MJ. The Trabecular Meshwork: A Basic Review of Form and Function. *J Ocul Biol Dis Infor*. 2014;2(1). <https://www.ncbi.nlm.nih.gov/pubmed/25356439>.
34. Nakajima E, Nakajima T, Minagawa Y, Shearer TR, Azuma M. Contribution of ROCK in contraction of trabecular meshwork: proposed mechanism for regulating aqueous outflow in monkey and human eyes. *J Pharm Sci*. 2005;94(4):701-708.
35. Doornaert B, Leblond V, Planus E, et al. Time course of actin cytoskeleton stiffness and matrix adhesion molecules in human bronchial epithelial cell cultures. *Exp Cell Res*. 2003;287(2):199-208.
36. Wang K, Read AT, Sulchek T, Ethier CR. Trabecular meshwork stiffness in glaucoma. *Exp Eye Res*. 2017;158:3-12.
37. Calzado-Martín A, Encinar M, Tamayo J, Calleja M, San Paulo A. Effect of Actin Organization on the Stiffness of Living Breast Cancer Cells Revealed by Peak-Force Modulation Atomic Force Microscopy. *ACS Nano*. 2016;10(3):3365-3374.
38. Raghunathan VK, Morgan JT, Park SA, et al. Dexamethasone Stiffens Trabecular Meshwork, Trabecular Meshwork Cells, and Matrix. *Invest Ophthalmol Vis Sci*. 2015;56(8):4447-4459.
39. Gavara N, Chadwick RS. Relationship between cell stiffness and stress fiber amount, assessed by simultaneous atomic force microscopy and live-cell fluorescence imaging. *Biomech Model Mechanobiol*. 2016;15(3):511-523.
40. Morgan JT, Raghunathan VK, Chang Y-R, Murphy CJ, Russell P. The intrinsic stiffness of human trabecular meshwork cells increases with senescence. *Oncotarget*. 2015;6(17):15362-15374.
41. Peng J, Feng X-Y, Ye Z-M, et al. Effects of dexamethasone and HA1077 on actin cytoskeleton and β -catenin in cultured human trabecular meshwork cells. *Int J Ophthalmol*. 2016;9(10):1376-1380.
42. Clark AF, Brotchie D, Read AT, et al. Dexamethasone alters F-actin architecture and promotes cross-linked actin network formation in human trabecular meshwork tissue. *Cell Motil Cytoskeleton*. 2005;60(2):83-95.
43. Rao PV, Deng PF, Kumar J, Epstein DL. Modulation of aqueous humor outflow facility by the Rho kinase-specific inhibitor Y-27632. *Invest Ophthalmol Vis Sci*. 2001;42(5):1029-1037.
44. Rao PV, Deng P, Sasaki Y, Epstein DL. Regulation of myosin light chain phosphorylation in the trabecular meshwork: role in aqueous humour outflow facility. *Exp Eye Res*. 2005;80(2):197-206.
45. Zhang M, Rao PV. Blebbistatin, a novel inhibitor of myosin II ATPase activity, increases aqueous humor outflow facility in perfused enucleated porcine eyes. *Invest Ophthalmol Vis Sci*. 2005;46(11):4130-4138.
46. Honjo M, Inatani M, Kido N, et al. A myosin light chain kinase inhibitor, ML-9, lowers the intraocular pressure in rabbit eyes. *Exp Eye Res*. 2002;75(2):135-142.
47. Rao PV, Deng P, Maddala R, Epstein DL, Li C-Y, Shimokawa H. Expression of dominant negative Rho-binding domain of Rho-kinase in organ cultured human eye anterior segments increases aqueous humor outflow. *Mol Vis*. 2005;11:288-297.
48. May RC, Machesky LM. Phagocytosis and the actin cytoskeleton. *J Cell Sci*. 2001;114(Pt 6):1061-1077.

49. Mannherz HG. *The Actin Cytoskeleton and Bacterial Infection*. Springer; 2017.
50. Rohen JW, van der Zypen E. The phagocytic activity of the trabecular meshwork endothelium. *Albrecht von Graefes Arch Klin Ophthalmol*. 1968;175(2):143-160.
51. Matsumoto Y, Johnson DH. Dexamethasone decreases phagocytosis by human trabecular meshwork cells in situ. *Invest Ophthalmol Vis Sci*. 1997;38(9):1902-1907.
52. Castellano F, Le Clainche C, Patin D, Carlier M, Chavrier P. A WASp–VASP complex regulates actin polymerization at the plasma membrane. *EMBO J*. 2001;20(20):5603-5614.
53. McMenamin PG, Steptoe RJ. Normal anatomy of the aqueous humour outflow system in the domestic pig eye. *J Anat*. 1991;178:65-77.
54. Camras LJ, Stamer WD, Epstein D, Gonzalez P, Yuan F. Differential effects of trabecular meshwork stiffness on outflow facility in normal human and porcine eyes. *Invest Ophthalmol Vis Sci*. 2012;53(9):5242-5250.
55. Dang Y, Kaplowitz K, Parikh HA, et al. Steroid-induced glaucoma treated with trabecular ablation in a matched comparison with primary open-angle glaucoma. *Clin Experiment Ophthalmol*. 2016;44(9):783-788.
56. Loewen RT, Roy P, Parikh HA, Dang Y, Schuman JS, Loewen NA. Impact of a Glaucoma Severity Index on Results of Trabectome Surgery: Larger Pressure Reduction in More Severe Glaucoma. *PLoS One*. 2016;11(3):e0151926.
57. Roy P, Loewen RT, Dang Y, Parikh HA, Bussell II, Loewen NA. Stratification of phaco-trabectome surgery results using a glaucoma severity index in a retrospective analysis. *BMC Ophthalmol*. 2017;17(1):30.
58. Akil H, Chopra V, Huang A, Loewen N, Noguchi J, Francis BA. Clinical Results of Ab Interno Trabeculotomy Using the Trabectome in Patients with Pigmentary Glaucoma compared to Primary Open Angle Glaucoma. *Clin Experiment Ophthalmol*. March 2016. doi:10.1111/ceo.12737.